Published by IOP Publishing for Sissa Medialab

Received: *February 26, 2026*
Accepted: *March 19, 2026*
Published: *May 5, 2026*

Light Detection In Noble Elements (LIDINE 2025)
Hong Kong, China
21–24 October 2025

Imaging of scintillation light with coded aperture masks

L. Basiricò[a], **V. Cicero**[b,*], **E. Colantoni**[a], **G. De Matteis**[c], **L. Martina**[c], **N. Mauri**[a], **V. Pia**[b] **and N. Tosi**[b]

[a] *Department of Physics and Astronomy "Augusto Righi", Università di Bologna, Viale Carlo Berti Pichat 6/2, Bologna, Italy*
[b] *Istituto Nazionale di Fisica Nucleare, Sezione di Bologna, Viale Carlo Berti Pichat 6/2, Bologna, Italy*
[c] *Department of Mathematics and Physics "Ennio De Giorgi", Università del Salento, Via per Arnesano, Lecce, Italy*

E-mail: valentina.cicero@bo.infn.it

Abstract: Large volumes of liquid argon or xenon constitute an excellent medium for the detection of Neutrino interactions and for Dark Matter searches. Traditionally, noble liquid detectors use scintillation light for a timing or calorimetric signal, read out in a time projection chamber configuration, where the liquid is permeated by an electric field. A direct optical reconstruction of the events though the imaging of scintillation light may offer an alternative to charge collection, removing the need for an electric drift field and the associated high-voltage hardware. Using finely segmented silicon photomultipliers arrays and a suitable optical system, it becomes possible to construct cameras that effectively "photograph" the primary scintillation light. A major challenge arises from the fact that both argon and xenon scintillate in the vacuum-ultraviolet range. To address this, we employ coded aperture masks in place of traditional lenses, enabling thin cameras with wide and deep field of view. A reconstruction algorithm based on Maximum Likelihood Expectation Maximization has been developed to obtain a 3D map of energy deposition, outperforming traditional deconvolution techniques in simulation under low-light conditions. The latest results from simulation and reconstruction of neutrino interactions in a liquid argon detector equipped with these cameras will be presented.

Keywords: Data processing methods; Noble liquid detectors (scintillation, ionization, double-phase); Neutrino detectors; Photon detectors for UV, visible and IR photons (solid-state) (PIN diodes, APDs, Si-PMTs, G-APDs, CCDs, EBCCDs, EMCCDs, CMOS imagers, etc)

*Corresponding author.

https://doi.org/10.1088/1748-0221/21/05/C05001

Contents

2026 JINST 21 C05001

1 Introduction

Noble-liquid detectors are widely used in experiments for dark-matter detection [1] and neutrino physics [2], and proposals exist for their application in medical imaging [3]. Most noble-liquid detectors are read out using the time projection chamber technique, which combines collection of drift charge with detection of scintillation light. This approach yields excellent spatial and energy resolution; its only intrinsic drawback is the relatively slow charge drift time. While this limitation can be safely ignored in detectors searching for rare decays, accelerator-based neutrino experiments and other high-rate applications benefit from, and sometimes require, faster readout.

Direct optical imaging of scintillation light with cameras offers an alternative to charge collection. Recording photons from multiple viewing angles enables spatial reconstruction, while the achievable event rate is essentially limited only by the scintillation-decay timescale. An optical detector of this type eliminates the need for an electric drift field and the associated high-voltage hardware, improving mechanical and operational robustness.

However, imaging the scintillation of liquid argon or xenon presents significant challenges because their emission lies in the vacuum-ultraviolet (VUV) band [4]. Standard lens-plus-CMOS camera systems are unsuitable for direct VUV scintillation imaging: they lack sufficient sensitivity and aperture. We instead implement dense arrays of silicon photomultipliers (SiPMs) as the photosensing planes, which provide fine spatial segmentation for the detection of images. Moreover, SiPM matrices operated at cryogenic temperatures provide single-photon sensitivity with greatly reduced dark-count rates and reliable operation. The individual pixels are coated with a wavelength shifter to convert VUV photons to wavelengths matching the SiPM photon-detection efficiency (PDE).

The choice of an optical system for this camera is not trivial. Constructing a lens system that offers adequate aperture, width, and depth of field while remaining sufficiently transparent to VUV light is difficult. We therefore introduce an alternative: *coded aperture masks*, optical aperture-modulating elements that encode spatial information and are widely used in astronomy and X-ray imaging.

2 Coded aperture imaging

The coded-aperture concept was originally developed in the context of X-ray astronomy [5] as an extension of the pinhole camera. A simple pinhole camera consists of an opaque barrier that separates the detector plane from the radiation source and a single small aperture that permits light or radiation to pass through. A pinhole camera can achieve excellent angular resolution, but it is intrinsically inefficient because most incident photons are blocked by the opaque material, producing substantial count loss.

Coded-aperture imaging was introduced to retain the angular resolution of a pinhole while substantially improving detection efficiency. Instead of a single aperture in an attenuating plane, a mask formed from an array of opaque and transparent elements is placed between the incoming flux and a position-sensitive detection plane. These transparent and opaque elements, are all of equal size and are arranged in a predetermined pattern on a regular grid; the individual cell shape may be chosen to suit application-specific constraints.

Each point within the field of view projects a shadow of the mask onto the detection plane. For an isolated point source, the detected two-dimensional distribution reproduces the mask pattern (or a portion of it), but shifted from the central position by an amount that is uniquely related to the source position. For extended sources or multiple point sources, the recorded data is the linear superposition of the individual shifted mask patterns produced by each source element. Figure 1 shows a schematic comparison of a pinhole camera and a coded-aperture camera.

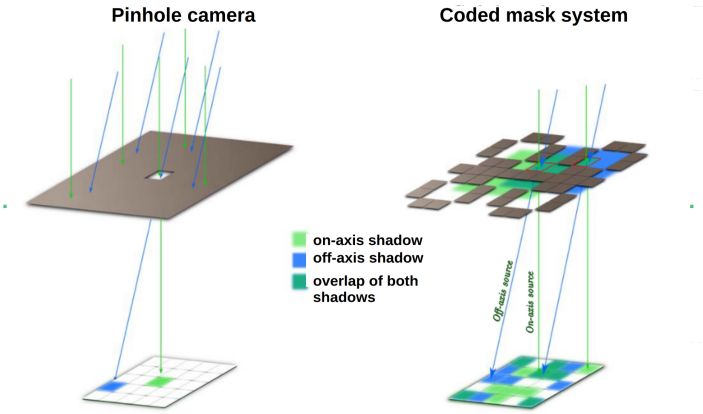

Figure 1. Schematic comparison of a pinhole and a Coded Aperture Mask camera.

3 Reconstruction

The reconstruction of the source distribution from sensor data can be performed with a variety of methods and algorithms [6]. In this work we apply the *Maximum Likelihood Expectation Maximization* (ML-EM) algorithm [7].

In the ML-EM algorithm, the data are treated as samples from a set of random variables whose probability density functions are related to the source distribution according to a model of the light propagation and detection process. Using this model, it is possible to calculate the probability that any initial distribution density in the light source under study could have produced the observed data. In the set of all possible distributions the one having the highest such probability is the *maximum likelihood* estimate of the original object.

This ML estimate λ is calculated iteratively over a discretized grid of voxels (denoted by index j), starting from the amplitude data for each sensor $h(s)$ using the following expression:

$$\lambda^{(k+1)}(j) = \lambda^{(k)}(j) \cdot \sum_s \frac{h(s)\widetilde{p}(j,s)}{\sum_{j'} \lambda^{(k)}(j')\widetilde{p}(j',s)} \tag{3.1}$$

where $\lambda^{(k)}$ is the estimate of λ at the *k-th* iteration, and $\lambda^{(0)}$ is a non-negative prior distribution, which can be assumed constant in absence of other information. The model of the scintillation process is

2026 JINST 21 C05001

contained in the $\widetilde{p}(j,s)$ *system matrix*, which consist of the probability $p(j,s)$ that light emitted in voxel j of the active material is detected in sensor s, normalized to one:

$$\widetilde{p}(j,s) = \frac{p(j,s)}{\sum_s p(j,s)}\,, \qquad \sum_s \widetilde{p}(j,s) = 1\,. \tag{3.2}$$

At every iteration $\sum_j \lambda^k(j)$ is conserved, and the event reconstruction is obtained as a final step after the *k-th* iteration with:

$$\lambda_{\text{reco}} = \frac{\lambda^{(k)}}{\sum_s p(j,s)}\,. \tag{3.3}$$

The system matrix for a realistic detector with thousands of channels can easily exceed one million elements, resulting in a substantial computational cost. The probability values can be calculated using Monte Carlo (MC) simulations by placing a point source in each voxel. However, given the long CPU time required by this method, we have opted to calculate probability values using some approximations that describe the physical process of detection, as described in detail in [8]. The probability that a photon emitted in voxel j is detected by sensor s is given by the product of:

- a geometric factor related to the viewing angle of the specific voxel-pixel pair, calculated as the solid angle originating at the center of the voxel and subtended by the portion of the sensor that is visible through the holes in the mask;
- an attenuation factor that depends on the absorption and scattering properties of the medium;
- the sensor detection efficiency.

4 Simulation of a liquid argon neutrino detector

For application in neutrino physics experiments, we simulated an example geometry of a detector with a cryostat of 150 cm × 150 cm × 50 cm, containing approximately 1 t of liquid argon. Neutrinos cross the detector horizontally. The cryostat is equipped with 60 cameras arranged as shown in the figure 2. Each cameras has a square array of 1024 SiPMs, and a opaque box with a pattern of square holes forming the mask. Both the sensors and the mask pixels have a 3 mm side and a 3.2 mm pitch, with the mask grid aligned to the sensor behind it, at a distance of 30 mm. Whether a mask cell is a hole or solid is assigned randomly, with half of the total area designated as solid. The mask pattern is the same in all cameras. A detailed discussion of the camera design optimization and performance is presented in [8].

We simulated 5000 ν_μ Charged-Current Quasi-Elastic (CCQE) interactions with ν_μ energy ranging from 1 to 4 GeV in the detector volume, using a simulation chain based on GENIE [9] for interaction generation in argon and Geant4 for scintillation-light production and propagation to the sensor plane. The collected photons, assuming a sensor PDE of 20% using SiPMs with a wavelength-shifter coating, constitute $h(s)$ in equation (3.1).

Event reconstruction with the ML-EM algorithm was performed with 200 fixed iterations and a discretization of the volume into 18 mm-side voxels. The system matrix was computed according to the approximations described. The algorithm was run on an NVIDIA H100 GPU, with an execution time of approximately 3 minutes per event.

An example reconstructed event is shown in figure 2. Voxels with values above a fixed threshold were selected and grouped using the DBSCAN clustering algorithm. The association of voxel clusters to different tracks was performed by comparison with the MC truth; development of track-finding

2026 JINST 21 C05001

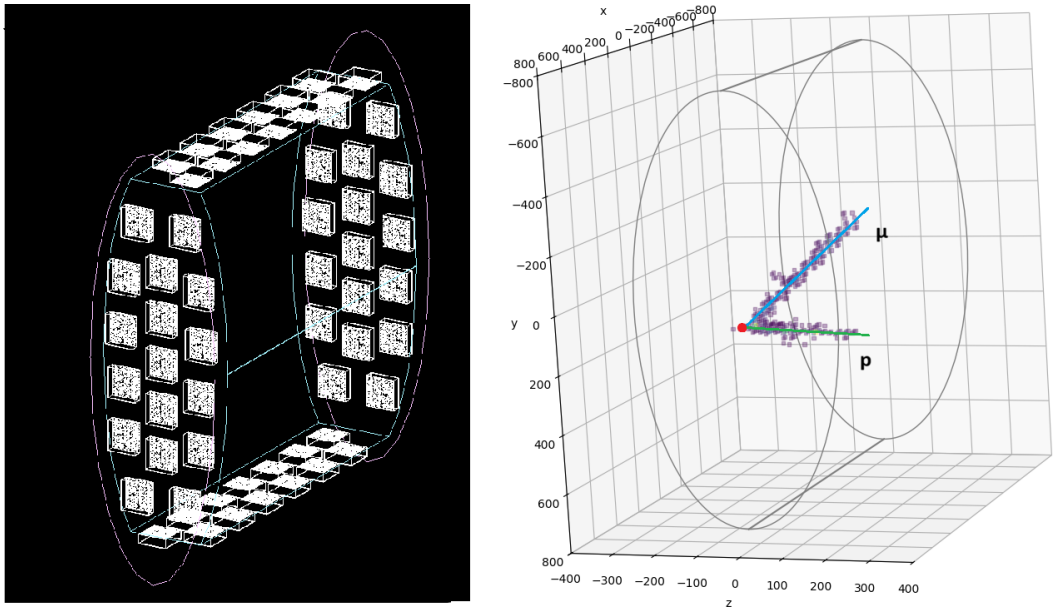

Figure 2. Left: Simulated geometry of a detector equipped with 60 coded aperture cameras, containing 1 t of liquid argon. Right: example reconstruction of a ν_μ CCQES on argon, producing a proton and a muon. The estimated voxelized photon density distribution is shown after a threshold cut. The vertex (red) and the produced particle trajectories (blue, green) are superimposed.

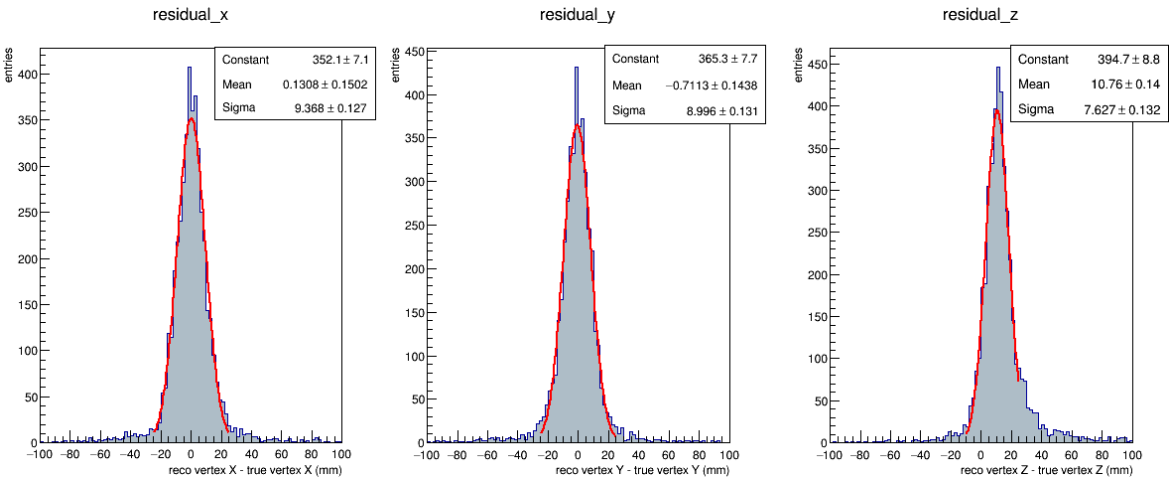

Figure 3. Residual distributions of the interaction vertex position along each axis.

algorithms is planned for future work. Clusters belonging to the same track were fitted with a 3D linear regression model to obtain the particle direction. As a figure of merit for reconstruction performance, the reconstructed vertex position is evaluated, computed as the intersection point of the fitted tracks. The distribution of the residuals between the position of the reconstructed vertex and the Monte Carlo truth is shown in figure 3. In all directions, the distribution exhibits a standard deviation of approximately 9 mm, consistent with the voxel sizes in the reconstruction. The bias in the distribution along the beam axis is attributed to the boosted topology of the simulated events and needs to be accounted for accordingly.

2026 JINST 21 C05001

5 Conclusion

The coded aperture masks readout technique for noble liquid detectors shows promise in simulation and the project is moving forward with the implementation of small scale prototypes. The present tracking performance is satisfactory but the algorithm runtime can be improved to cope with the high event rates. The use of this technique in future, larger, liquid argon detectors may be limited by the relatively short scattering length (~ 95 cm [10]) of the medium unless xenon doping is used or the volume segmented.

Acknowledgments

This work is part of the project "Imaging calorimetry in scintillating media for high energy physics and tomography" (PRIN 2022KJZSYB) and it is funded by the European Union Next Generation EU, Mission 4, Component 1, CUP I53D23001230006.

References

[1] T. Marrodán Undagoitia and L. Rauch, *Dark matter direct-detection experiments*, *J. Phys. G* **43** (2016) 013001 [arXiv:1509.08767].

[2] K. Majumdar and K. Mavrokoridis, *Review of Liquid Argon Detector Technologies in the Neutrino Sector*, *Appl. Sciences* **11** (2021) 2455 [arXiv:2103.06395].

[3] A. Zabihi et al., *3Dπ: three-dimensional positron imaging, a novel total-body PET scanner using xenon-doped liquid argon scintillator*, *Phys. Med. Biol.* **70** (2025) 065015.

[4] E. Segreto, *Properties of Liquid Argon Scintillation Light Emission*, *Phys. Rev. D* **103** (2021) 043001 [arXiv:2012.06527].

[5] E. Caroli et al., *Coded aperture imaging in X- and gamma-ray astronomy*, *Space Sci. Rev.* **45** (1987) 349.

[6] NU@FNAL collaboration, *Coded masks for imaging of neutrino events*, *Eur. Phys. J. C* **81** (2021) 1011 [arXiv:2105.10820].

[7] Y. Vardi, L.A. Shepp and L. Kaufman, *A Statistical Model for Positron Emission Tomography*, *J. Am. Statist. Assoc.* **80** (1985) 8.

[8] V. Cicero, *Study of the tracking performance of a liquid Argon detector based on a novel optical imaging concept*, Ph.D. Thesis, Alma Mater Studiorum, Università di Bologna, Bologna, Italy (2023) [DOI:10.48676/unibo/amsdottorato/10871].

[9] C. Andreopoulos et al., *The GENIE Neutrino Monte Carlo Generator*, *Nucl. Instrum. Meth. A* **614** (2010) 87 [arXiv:0905.2517].

[10] G.M. Seidel, R.E. Lanou and W. Yao, *Rayleigh scattering in rare gas liquids*, *Nucl. Instrum. Meth. A* **489** (2002) 189 [hep-ex/0111054].

2026 JINST 21 C05001